Review of Scientific Instruments ARTICLE scitation.org/journal/rsi

Cryostat setup for measuring spectral and electrical properties of light-emitting diodes at junction temperatures from 81 K to 297 K

Cite as: Rev. Sci. Instrum. 91, 015106 (2020); doi: 10.1063/1.5125319
Submitted: 22 August 2019 • Accepted: 16 December 2019 •
Published Online: 3 January 2020

Elvira Martikainen,[1,a)] Anna Vaskuri,[1,b)] Timo Dönsberg,[1,2] and Erkki Ikonen[1,2]

AFFILIATIONS

[1] Metrology Research Institute, Aalto University, P.O. Box 15500, 00076 Aalto, Finland
[2] VTT MIKES, VTT Technical Research Centre of Finland Ltd., P.O. Box 1000, 02044 VTT Espoo, Finland

[a)] **E-mail:** elvira.martikainen@aalto.fi
[b)] **Current address:** National Institute of Standards and Technology, Boulder, CO, USA.

ABSTRACT

We introduce a cryostat setup for measuring fundamental optical and electrical properties of light-emitting diodes (LEDs). With the setup, the cryostat pressure and the LED properties of the forward voltage, junction temperature, and electroluminescence spectrum are monitored with temperature steps less than 1.5 K, over the junction temperature range of 81–297 K. We applied the setup to commercial yellow AlGaInP and blue InGaN LEDs. At cryogenic temperatures, the fine structure of the electroluminescence spectra became resolved. For the yellow LED, we observed the phonon replica at 2.094 eV that was located 87 meV below the peak energy at the junction temperature of 81 K. For the blue LED, we observed the cascade phonon replicas at 2.599 eV, 2.510 eV, and 2.422 eV with the energy interval of 89 meV. For both LED types, the forward voltage increased sharply toward the lower temperatures due to the increased resistivity of materials in the LED components. We found significant differences between the temperature dependent behaviors of the forward voltages, spectral peak energies, and bandgap energies of LEDs obtained from the Varshni formula. We also noted a sharp pressure peak at 180–185 K arising from the solid-vapor phase transition of water when the base level of the cryostat pressure was approximately 0.4 mPa.

I. INTRODUCTION

Applications relying on opto-semiconductors cover, for example, light-emitting diodes (LEDs), lasers, optical detectors, and solar cells. A major factor limiting their efficiency is the junction temperature. For this reason, it is important to understand the junction temperature dependence of their spectral and electrical properties. One effective way to observe changes in the junction temperature is to monitor the electroluminescence or photoluminescence spectra of direct bandgap semiconductors. The observed shift in the spectral peak energy of an LED spectrum originates from the change in interatomic distances that directly affects the bandgap energy.[1] At low temperatures, lattice vibrations become a less dominating feature in the spectra, revealing the fine structure of the joint density of states that is closely related to the periodic energy band structure for high quality crystalline semiconductors. For example, the band offsets of the material can be determined from spectral measurements at extremely low temperatures.[2–4]

The temperature dependence of semiconductors has been extensively studied over the years.[2,3,5–7] Also, new ways to determine the junction temperature from LED spectra have been studied, for example, by Vaitonis *et al.*,[8] Chen and Narendran,[9] He *et al.*,[10] Keppens *et al.*,[11] and Chou and Yang.[12] These models either are empirical or can only model a narrow part of the spectrum as they neglect broadening of the joint density of states. Recently, Vaskuri *et al.*[13,14] have proposed more accurate models to overcome the limitations of the simplified approaches. These new models allow for estimating the junction temperature from electroluminescence spectra of red and blue LEDs with the standard uncertainty better than 4 K at the temperature range of 303–398 K. In addition, for example,

Feldtmann *et al.*[15] provided a completely quantum mechanical approach to model spontaneous emission spectra. However, the method has not been used for estimating the junction temperatures of LEDs due to its complexity.

To understand the emission mechanisms in semiconductors, accurate spectral measurements over a large temperature range and with high temperature resolution are needed. In this paper, we report on a cryostat setup for studying spectral and electrical properties of LEDs, along with obtained measurement results (see the supplementary material). The careful implementation of the cryostat setup is important to obtain dense and reliable experimental data. In Sec. II, we introduce the cryostat setup for measuring the temperature dependence of semiconductors. We apply the setup to two commercial quantum-well LEDs made of AlGaInP (aluminum gallium indium phosphide) and InGaN (indium gallium nitride) by measuring their electroluminescence spectra with a few kelvin resolution at the junction temperatures from 81 K to 297 K. In Sec. III, we estimate how much higher the actual junction temperatures of the LEDs are compared to the heat sink temperatures measured in the cryostat setup. Results of electrical and spectral measurements are presented and analyzed in Sec. IV. From these data, we track the temperature dependence of the forward voltage and spectral peak energy and estimate the energies of phonon replicas for both LEDs. Conclusions are presented in Sec. V, emphasizing the scientific progress made in this work.

II. MEASUREMENT SETUP

The cryostat setup introduced in Fig. 1 includes a Wilmington MA01887 VPF 457 cryostat by Janis Research Co., Inc., and devices measuring following quantities with a 60 s interval: electroluminescence spectrum and forward voltage of LEDs, pressure in the vacuum chamber, and temperatures of a liquid nitrogen (N_2) reservoir and LEDs' holder. To achieve dense data over the 78–296 K temperature range, the measurement procedure was automated and measuring devices were operated in a remote mode by the custom-made LabVIEW software. The LEDs used in experiments are manufactured by Osram and belong to the Golden DRAGON Plus family. The yellow AlGaInP LED is based on the Thinfilm AlGaInP technology,[16] and the blue InGaN LED is based on the ThinGaN technology.[17] To reduce the number of cryostat disassemblies, LEDs were mounted on the opposite side of the metal holder plate, as shown in Fig. 1(c), inside the cryostat chamber.

The cryostat setup was implemented as an open loop system with a temperature response [Fig. 2(a)] being affected mainly by natural heating after complete evaporation of liquid nitrogen (N_2) used for cooling the cryostat down to 78 K. The step response of the heat sink temperature inside the cryostat is

$$T(t) = 78.55\ \mathrm{K} + 224.24\ \mathrm{K} \cdot \left(1 - e^{-t/\tau}\right), \tag{1}$$

where $\tau = 2.24$ h is the time constant of the system. Measured responses and the corresponding first-order model presented as a solid black curve are shown in Fig. 2(a). A relatively long time constant of the system and measurements every 60 s with a maximum temperature difference of 1.48 K at the beginning of the step response enable us to gather wide range and high-resolution data for analysis.

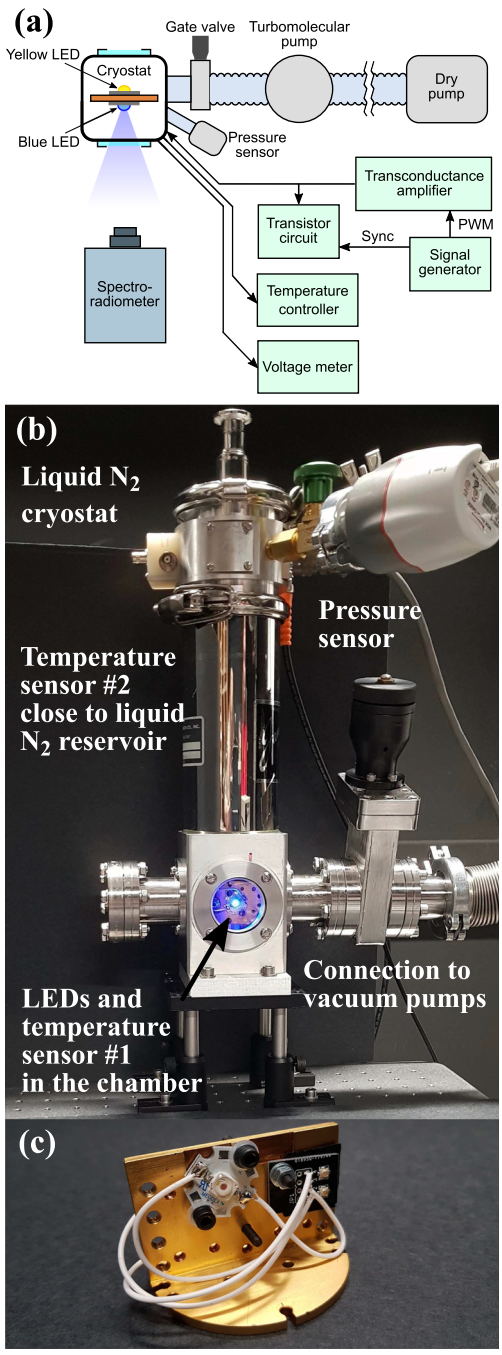

FIG. 1. Schematic diagram (a) and a photograph (b) of the cryostat setup for measuring LEDs and a holder plate for LEDs to be placed inside the vacuum chamber (c).

Temperature was measured with a Lake Shore 325 cryogenic temperature controller and silicon diode temperature sensors suitable for measurements in cryogenic and room temperatures. Temperature sensor No. 1 was attached to a metal holder plate alongside

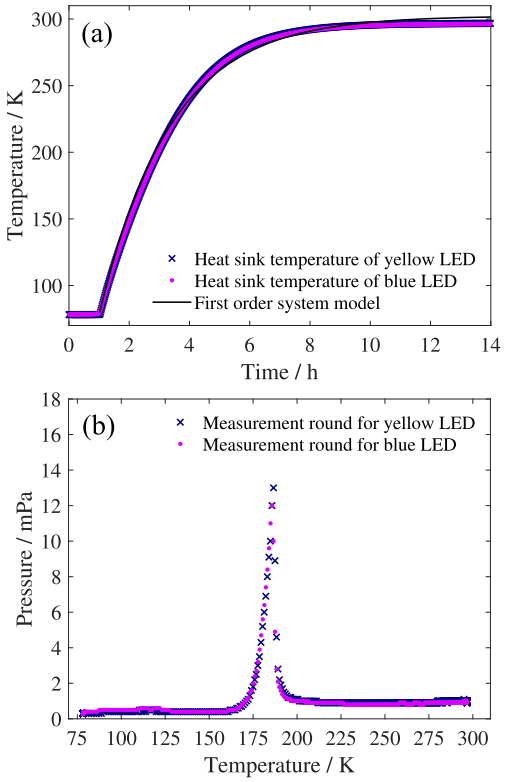

FIG. 2. Open loop step response of the cryostat setup (a) and the pressure inside the vacuum chamber as a function of the heat sink temperature (b). The solid-vapor phase transition of water is responsible for a sharp peak in the pressure at 180–185 K.[19]

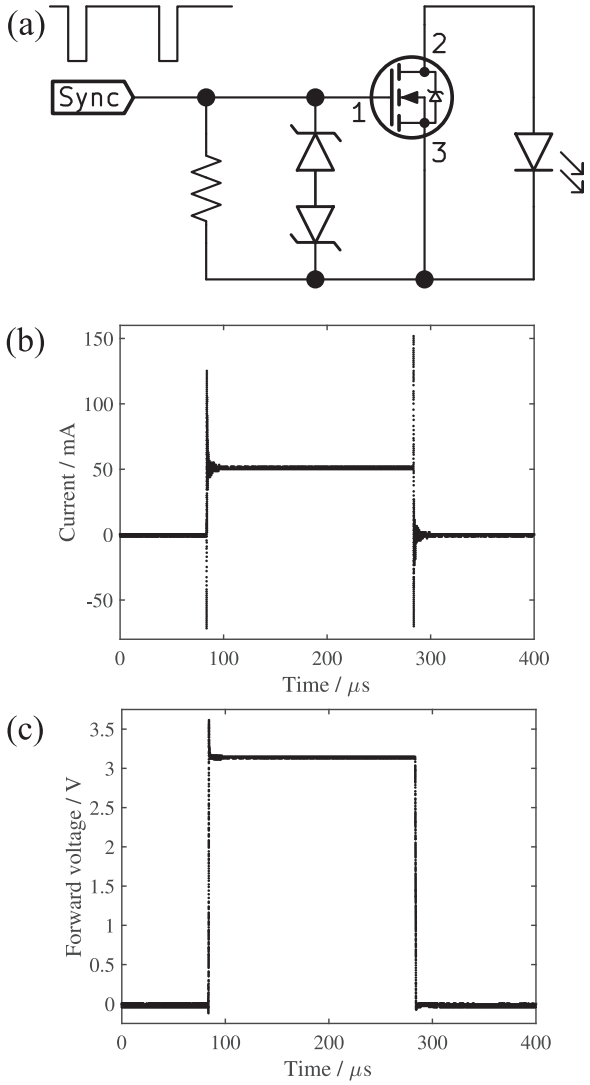

FIG. 3. Schematic diagram of the transistor circuit (a), the current pulse through a blue InGaN LED (b), and the corresponding forward voltage over the blue InGaN LED (c). In (a), the circuit consists of an N-channel MOSFET transistor (model PSMN2R0-30PL) with a 1 MΩ resistor and two Zener diodes for protecting the transistor against overshoot transients.

the LEDs, and temperature sensor No. 2 was located near the cryostat reservoir [Fig. 1(b)]. The temperature difference between sensors' readings was less than 0.36 K for both LEDs throughout the measurements. The method for obtaining the junction temperature of the LED from the heat sink temperature readings of sensor No. 1 is discussed in Sec. III.

Due to the strong temperature dependence of the forward voltage, LEDs were operated in a pulsed current mode, which also purposely minimizes the heating of the LED junction. A custom-made transconductance amplifier[18] was used as a current source for LEDs. The gain of the transconductance amplifier was set to 0.1 A/V, and the input of the amplifier was driven by the pulse width modulated (PWM) voltage generated by the Agilent 33521A Function waveform generator. The rectangular waveform voltage was set to 0.5 V peak-to-peak amplitude, 0.25 V offset, 1 kHz frequency, and 20% duty cycle. The output current shown in Fig. 3(b) has a rectangular waveform with 0–50.03 mA amplitude, and frequency and duty cycle corresponding to those of the input voltage signal. The low duty cycle ensures that the junction temperature is close to that measured by sensor No. 1. In our setup, even a small voltage offset in the function generator input is converted to a notable current level in the output that switches on the LED. To ensure the LED is completely switched either ON or OFF, a transistor circuit shown in Fig. 3(a) is connected in parallel with the LED. During the OFF state of the LED current pulse, a synchronization signal (Sync) is kept well above the MOSFET threshold, and during the ON state, the synchronization signal is grounded. This technique forces the LED current to zero when the pulse is down enabling to measure the average forward voltage over many pulses that can be converted to the true forward voltage by multiplication with the inverse of the duty cycle. With the duty cycle of 20%, the forward voltage is obtained as $V_f = V_{meas}/0.2$, where V_{meas} is the average forward voltage of an LED measured with the Agilent digital multimeter 34410A using 100 NPLCs (number of power-line cycles) that corresponds to averaging over 2 s. The

forward voltage waveform over the blue InGaN LED is shown in Fig. 3(c).

In order to prevent icing, near-vacuum conditions inside the cryostat were obtained and maintained with the dry pump XDS5 and turbomolecular pump EXT75DX NW40 with TIC Turbo Controller 100W by EDWARDS. The turbomolecular pump was connected between the cryostat and the dry pump compressing the gas and moving it out of the cryostat. The dry pump kept the background pressure low and drew gas out of the pump system. Pressure inside the cryostat was measured with an EDWARDS active digital controller and a pressure sensor located near the liquid N_2 reservoir. The pressure vs temperature curve is displayed in Fig. 2(b). The peak in the pressure-temperature curve occurs approximately at 180–185 K, which is attributed to the phase transition of water from the solid to the vapor form.[19]

Electroluminescence spectra of the LEDs studied were measured with a calibrated CS-2000A spectroradiometer by Konica Minolta with the step size of 1 nm at the wavelength range of 380–780 nm. Measurements were made in the irradiance mode (W m^{-2} nm^{-1}) with a diffuser being attached to the objective. The distance between the diffuser and the LED under measurement was 45–50 cm.

III. JUNCTION TEMPERATURE ESTIMATION

In the experiments, junction temperatures were determined indirectly by measuring the temperatures of a holder plate, i.e., heat sink temperatures. Therefore, additional tests were performed on LEDs to determine how much higher the junction temperatures are compared to the heat sink temperatures. We traced the behavior of the forward voltage in order to spot possible changes in its waveform associated with a change in junction temperature.

During tests, a rectangular current pulse of 0–50.03 mA with the pulse width of 100 ms was passed through LEDs every 10 s to avoid heating the junction. The output terminal of the amplifier was connected in parallel with a 1 kΩ resistor, when performing these measurements to eliminate the overshoot at the beginning of each pulse that is shown in Figs. 3(b) and 3(c) as it is not related to the changing junction temperature. 30 rounds of measurements were taken by a Hewlett Packard 3458A multimeter, with one round consisting of 5000 samples of the forward voltage separated with the time steps of 20 μs. Averaged pulses at the heat sink temperatures of 296 K [(a) and (c)] and 78 K [(b) and (d)] are plotted as a function of the square root of time in Fig. 4, as specified in the technical report CIE 225:2017 by Commission Internationale de l'Eclairage.[20] The forward voltages drop as a result of current-induced heating of the junction, showing mild slopes and small shifts of 0.91% at 78 K and 0.046% at 296 K for the yellow LED and 0.82% at 78 K and 0.095% at 296 K for the blue LED, respectively. These forward voltage changes indicate that the junction temperatures are 3.59 K and 0.66 K, and 2.60 K and 1.59 K higher than the heat sink temperatures for the yellow and blue LEDs at 78 K and 296 K, respectively. We expect a linear dependence between the junction and heat sink temperatures over 78–296 K so that the results in Sec. IV are given as a function of the junction temperature.

IV. RESULTS

The temperature evolutions of electroluminescence spectra of blue InGaN and yellow AlGaInP LEDs are shown in Fig. 5. The spectral irradiances $E_\lambda(\lambda)$ were originally measured as a function of wavelength (W m^{-2} nm^{-1}) using a calibrated spectroradiometer. In order to observe physical phenomena from the temperature evolutions in Fig. 5, the spectra have been plotted as a function of photon energy,

$$\hbar\omega = \frac{hc}{n\lambda}, \tag{2}$$

where h is Planck's constant, c is the speed of light in vacuum, n is the refractive index of air, and λ is the photon wavelength in air. Due to the inversion of the horizontal scale, we converted spectral irradiance to the spectral photon rate (photons m^{-2} s^{-1} eV^{-1}) with

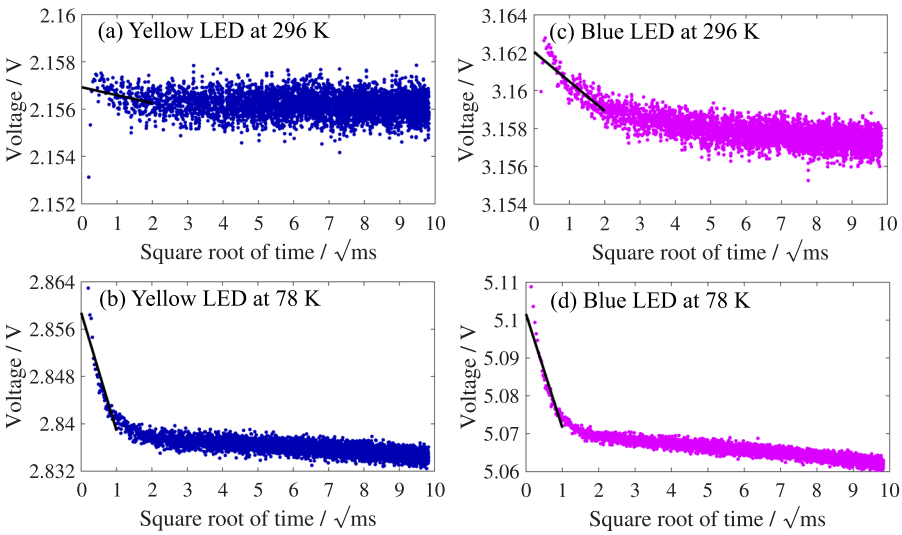

FIG. 4. Average of 30 forward voltage pulses as a function of the square root of time measured at the heat sink temperatures of 78 K and 296 K for a yellow LED [(a) and (b)] and a blue LED [(c) and (d)]. The forward voltages are back extrapolated to the beginning of the pulses (black solid lines) at the square root of the time scale, according to the technical report CIE 225:2017.[20] The decreasing forward voltage corresponds to the rising junction temperature. Thus, the differences between the heat sink and junction temperatures can be estimated from the voltage drops.

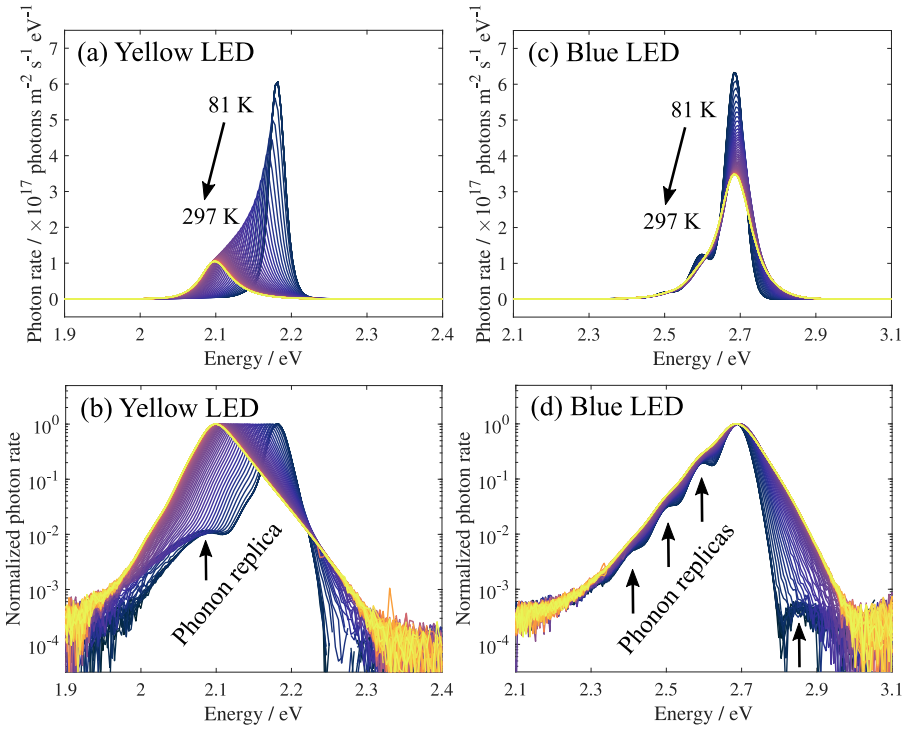

FIG. 5. Every 10th electroluminescence spectrum of a yellow AlGaInP LED [(a) and (b)] and a blue InGaN LED [(c) and (d)] measured with the cryostat setup over the junction temperatures from 81 K to 297 K. Spectra are plotted both on a linear scale in [(a) and (c)] and on a logarithmic scale (b) and (d). Phonon replicas, indicated by arrows in [(b) and (d)], are clearly observed in the logarithmic spectra.

the following equation:

$$r(\hbar\omega) = \frac{hc}{(\hbar\omega)^3} \cdot E_\lambda(\lambda). \tag{3}$$

This conversion changes only slightly the shape of narrow bandwidth spectra measured in this study.

Spectral broadening accompanied by a decrease in the spectral photon rate is observed with increasing temperature, as shown in Fig. 5. Electroluminescence spectra broaden at higher temperatures due to increased thermal excitation of electrons and also due to broadening of the density of states.[6] Phonon replicas are characteristic of the strong phonon-exciton coupling, and they have been noted earlier for InGaN at least by Smith *et al.*,[21] Ozaki *et al.*,[22] Kovalev *et al.*,[23] and Paskov *et al.*[5] The commercial InGaN LED spectra studied in this work also reveal a cascade structure of first-, second-, and third-order phonon replicas with an 89 meV interval located at the energies of 2.599 eV, 2.510 eV, and 2.422 eV, respectively. The excitons are created due to uneven clustering of indium across the InGaN LED chip arising from the lattice mismatch between InN and GaN.[24,25] The high energy side of the InGaN spectra contains a replica at 2.877 eV with 189 meV energy. AlGaInP spectra have a distinct phonon replica at 2.094 eV that is 87 meV below the spectral peak energy at the junction temperature of 81 K. As the temperature increases, the phonon replicas merge and become unresolved due to the exciton delocalizations and in the case of AlGaInP LED also due to the suppression of the band edge.

The optical and electrical characteristics of the LEDs studied are plotted as a function of the junction temperature in Fig. 6. The junction temperatures were determined from the heat sink temperatures using the forward voltage method described in detail in Sec. III. For the yellow LED, red-shift in the main peak energies was observed toward higher junction temperatures in Fig. 6. The peak energy decreases systematically with increasing temperature. The peak energy of the blue InGaN LED shifts only slightly with temperature. The blue-shift of the InGaN spectral peak is observed at low junction temperatures up to 240 K. This is a turning point after which the spectral peak red-shifts toward higher junction temperatures.[5–7,26] The standard deviations in the spectral peak energies from the averaged values are 280 μeV for the blue InGaN LED and 70 μeV for the yellow AlGaInP LED.

In contrast to the peak energies, the bandgap energies E_g obey the Varshni formula and alloy mixing equations collected in the articles by Vurgaftman *et al.*[2,3] The alloy mixing ratio of the blue LED was estimated to be $In_{0.18}Ga_{0.82}N$. The quantum-well layers of the yellow LED were estimated to be grown on a gallium arsenide (GaAs) substrate and thus expected to be lattice matched to GaAs as follows: $(Al_{0.33}Ga_{0.67})_{0.51}In_{0.49}P$. The theoretical bandgap energies for both LEDs are presented as dashed curves in Fig. 6.

Forward voltage curves are presented in Fig. 6. Forward voltage decreases with increasing temperature showing two-slope characteristics with a steeper slope appearing at cryogenic temperatures and a milder slope starting approximately at 150–175 K. At cryogenic temperatures, the slopes $\Delta V_f/\Delta T$ are −7.498 mV/K and −16.317 mV/K for the yellow and blue LEDs, respectively. Increasing forward voltages toward cryogenic temperatures have earlier been measured for InGaN LEDs by Meyaard *et al.*,[27] and according to them, the effect is associated with the increment of series and contact resistances of an LED due to decreased mobility of the holes toward cryogenic temperatures. In this study, we have confirmed that the AlGaInP LEDs follow a similar behavior. The impact of the series resistance on the

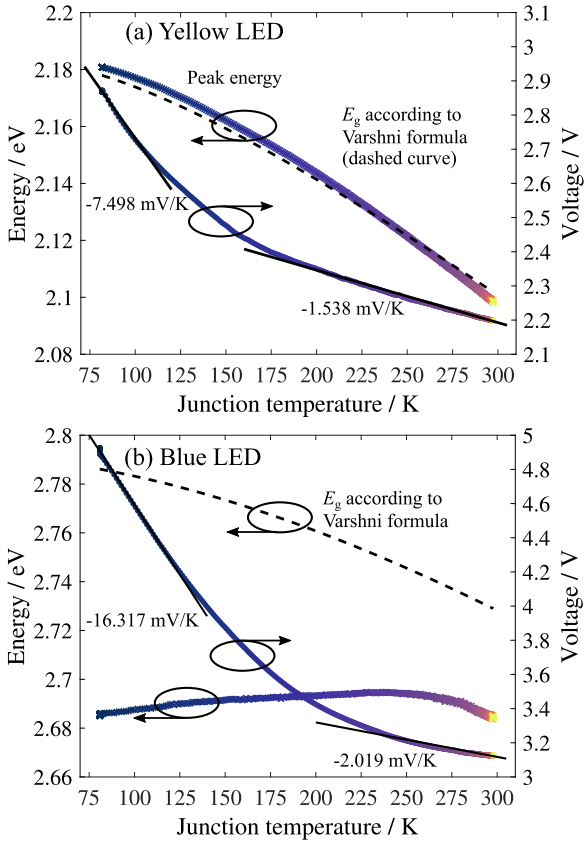

FIG. 6. Peak energies of the electroluminescence spectra and the forward voltages of a yellow AlGaInP LED (a) and a blue InGaN LED (b) as a function of the junction temperature. Dashed lines represent the dependences of the energy gap on junction temperature calculated with the Varshni formula[1] and alloy mixing equations.[2,3]

forward voltage at room temperature is significantly smaller,[27] and thus, the slopes are −1.538 mV/K and −2.019 mV/K for the yellow and blue LEDs at room temperature, respectively.

V. CONCLUSIONS

Our implementation of the cryostat setup enables collecting data with high temperature resolution in a wide range. High temperature resolution of the data measured in this work allows for fitting and testing the theoretical models without the need of interpolation. No datasets on LED spectra at cryogenic temperatures have been available prior to the supplementary material provided in this work. In order to develop real physical models for LED emission spectra, the models should work at all temperature regions, and we provide the dataset for such testing. A further important point is demonstrated in this work as if the heating at the beginning of the current pulse is not accounted for, a systematic error is introduced in the junction temperatures possibly affecting the validation of theoretical models for LED emission spectra.

In order to achieve a wider temperature range by heating, the open loop system of the setup can be closed with a Lake Shore proportional–integral–derivative (PID) temperature controller used in our experiments for temperature measurements. Due to the nature of the experiments, current is recommended for driving LEDs because of temperature variation of the forward voltage. For similar setups, with sensors not being directly attached to samples, we propose using pulsed current with a small duty cycle to reduce the contribution of current-generated heat to the measured temperature. The junction temperatures of the LEDs were maximally 3.6 K higher than the heat sink temperatures when the LEDs were driven by a rectangular current waveform of 0–50.03 mA.

We collected data at the junction temperature range of 81–297 K for further examination of the spectral and electrical properties of AlGaInP and InGaN LEDs. Both LEDs showed spectral broadening and a decrease in the spectral irradiance of the main and phonon replica generated peaks with increasing temperature. The peak energy of an electroluminescence spectrum does not correspond directly to the bandgap energy as it results from the joint density of states of the carriers that is weighted by their thermally induced occupation probabilities, i.e., Fermi–Dirac distributions. Due to the localized exciton-related broadening, i.e., cascade phonon replicas, we observed anomalous behavior of the peak energy shift with increasing temperature for the blue InGaN LED which did not follow the Varshni formula. Instead, the yellow AlGaInP LED spectra are created mainly by band-to-band recombinations, and thus, we observed red-shifting of the peak energy at the junction temperature range of 81–297 K according to the prediction of the Varshni formula. For both yellow and blue LEDs, the forward voltages followed series-resistance-induced two-slope characteristics with changing temperature. In conclusion, the spectral peak energy, bandgap energy, and forward voltage have completely different dependences on temperatures.

SUPPLEMENTARY MATERIAL

See the supplementary material for measurement data in the numerical form in URL.

ACKNOWLEDGMENTS

The authors thank Santeri Porrasmaa for the help with the vacuum pump system and Professor Tsung-Hsun Yang from National Central University, Taiwan, for useful discussions.

REFERENCES

[1] Y. P. Varshni, "Temperature dependence of the energy gap in semiconductors," Physica **34**, 149–154 (1967).
[2] I. Vurgaftman, J. R. Meyer, and L. R. Ram-Mohan, "Band parameters for III–V compound semiconductors and their alloys," Appl. Phys. Rev. **89**, 5815–5875 (2001).
[3] I. Vurgaftman and J. R. Meyer, "Band parameters for nitrogen-containing semiconductors," J. Appl. Phys. **94**, 3675–3696 (2003).
[4] D. C. Reynolds, D. C. Look, W. Kim, Ö. Aktas, A. Botchkarev, A. Salvador, H. Morkoç, and D. N. Talwar, "Ground and excited state exciton spectra from GaN grown by molecular-beam epitaxy," J. Appl. Phys. **80**, 594–596 (1996).
[5] P. P. Paskov, P. O. Holtz, B. Monemar, S. Kamiyama, M. Iwaya, H. Amano, and I. Akasaki, "Phonon-assisted photoluminescence in InGaN/GaN multiple quantum wells," Phys. Status Solidi B **234**, 755–758 (2002).

[6]H. Wang, Z. Ji, S. Qu, G. Wang, Y. Jiang, B. Liu, X. Xu, and H. Mino, "Influence of excitation power and temperature on photoluminescence in InGaN/GaN multiple quantum wells," Opt. Express **20**, 3932–3940 (2012).
[7]T. Langer, H.-G. Pietscher, F. A. Ketzer, H. Jönen, H. Bremers, U. Rossow, D. Menzel, and A. Hangleiter, "S shape in polar GaInN/GaN quantum wells: Piezoelectric-field-induced blue shift driven by onset of nonradiative recombination," Phys. Rev. B **90**, 205302-1–205302-9 (2014).
[8]Z. Vaitonis, P. Vitta, and A. Žukauskas, "Measurement of the junction temperature in high-power light-emitting diodes from the high-energy wing of the electroluminescence band," J. Appl. Phys. **103**, 093110-1–093110-7 (2008).
[9]K. Chen and N. Narendran, "Estimating the average junction temperature of AlGaInP LED arrays by spectral analysis," Microelectron. Reliab. **53**, 701–705 (2013).
[10]S. M. He, X. D. Luo, B. Zhang, L. Fu, L. W. Cheng, J. B. Wang, and W. Lu, "Junction temperature measurement of light emitting diode by electroluminescence," Rev. Sci. Instrum. **82**, 123101-1–123101-4 (2011).
[11]A. Keppens, W. R. Ryckaert, G. Deconinck, and P. Hanselaer, "Modeling high power light-emitting diode spectra and their variation with junction temperature," J. Appl. Phys. **108**, 043104-1–043104-7 (2010).
[12]H.-Y. Chou and T.-H. Yang, "Dependence of emission spectra of LEDs upon junction temperature and driving current," J. Light Vis. Environ. **32**, 183–186 (2008).
[13]A. Vaskuri, H. Baumgartner, P. Kärhä, G. Andor, and E. Ikonen, "Modeling the spectral shape of InGaAlP-based red light-emitting diodes," J. Appl. Phys. **118**, 203103-1–203103-7 (2015).
[14]A. Vaskuri, P. Kärhä, H. Baumgartner, O. Kantamaa, T. Pulli, T. Poikonen, and E. Ikonen, "Relationships between junction temperature, electroluminescence spectrum and ageing of light-emitting diodes," Metrologia **55**, S86–S95 (2018).
[15]T. Feldtmann, M. Kira, and S. W. Koch, "Phonon sidebands in semiconductor luminescence," Phys. Status Solidi B **246**, 332–336 (2009).
[16]Osram Opto Semiconductors, Golden DRAGON Plus, LR W5AM, LA W5AM, LY W5AM datasheet, 2009.
[17]Osram Opto Semiconductors, Golden DRAGON Plus, LB W5AM datasheet, 2013.
[18]T. Dönsberg, T. Poikonen, and E. Ikonen, "Transconductance amplifier for optical metrology applications of light-emitting diodes," IEEE Trans. Instrum. Meas. (published online).
[19]I. Bello, *Vacuum and Ultravacuum: Physics and Technology* (CRC Press, Boca Raton, FL, USA, 2017), p. 142, ISBN: 978-1-4987-8204-3.
[20]CIE 225:2017 Optical Measurement of High-Power LEDs, Commission Internationale de l'Eclairage, Vienna, Austria, 20171.
[21]M. Smith, J. Y. Lin, H. X. Jiang, A. Khan, Q. Chen, A. Salvador, A. Botchkarev, W. Kim, and H. Morkoc, "Exciton-phonon interaction in InGaN/GaN and GaN/AlGaN multiple quantum wells," Appl. Phys. Lett. **70**, 2882–2884 (1997).
[22]T. Ozaki, M. Funato, and Y. Kawakami, "Origin of temperature-induced luminescence peak shifts from semipolar (1122) $In_xGa_{1-x}N$ quantum wells," Phys. Rev. B **96**, 125305-1–125305-13 (2017).
[23]D. Kovalev, B. Averboukh, D. Volm, B. K. Meyer, H. Amano, and I. Akasaki, "Free exciton emission in GaN," Phys. Rev. B **54**, 2518–2522 (1996).
[24]S. Nakamura, "The roles of structural imperfections in InGaN based blue light-emitting diodes and laser diodes," Science **281**, 956–961 (1998).
[25]K. P. O'Donnell, R. W. Martin, and P. G. Middleton, "Origin of luminescence from InGaN diodes," Phys. Rev. Lett. **82**, 237–240 (1999).
[26]C.-C. Hung, H. Ahn, C.-Y. Wu, and S. Gwo, "Strong green photoluminescence from $In_xGa_{1-x}N$/GaN nanorod arrays," Opt. Express **17**, 17227–17233 (2009).
[27]D. S. Meyaard, J. Cho, E. F. Schubert, S.-H. Han, M.-H. Kim, and C. Sone, "Analysis of the temperature dependence of the forward voltage characteristics of GaInN light-emitting diodes," Appl. Phys. Lett. **103**, 121103-1–121103-4 (2013).